HHS Public Access

Author manuscript

J Heart Lung Transplant. Author manuscript; available in PMC 2024 April 01.

Published in final edited form as:

J Heart Lung Transplant. 2024 April ; 43(4): 594–603. doi:10.1016/j.healun.2023.11.015.

Occult right ventricular dysfunction and right ventricular-vascular uncoupling in left ventricular assist device recipients

Paul J Scheel III, MD[a,1], **Ilton M. Cubero Salazar, MD**[a], **Samuel Friedman, MD**[b], **Leora Haber, MD**[a], **Monica Mukherjee, MD**[a], **Matthew Kauffman, BS**[a], **Alexandra Weller, MD**[a], **Fatimah Alkhunaizi, MD**[a], **Nisha A. Gilotra, MD**[a], **Kavita Sharma, MD**[a], **Ahmet Kilic, MD**[b], **Paul M. Hassoun, MD**[c,d], **William K. Cornwell, MD**[e,f], **Ryan J. Tedford, MD**[g], **Steven Hsu, MD**[a,2]

[a]Division of Cardiology, Department of Medicine, Johns Hopkins University School of Medicine, Baltimore, Maryland

[b]Division of Pulmonary, Critical Care, Allergy and Sleep Medicine, Department of Medicine, Medical University of South Carolina, Charleston, South Carolina

[c]Division of Cardiothoracic Surgery, Department of Surgery, Johns Hopkins University School of Medicine, Baltimore, Maryland

[d]Division of Pulmonary and Critical Care, Department of Medicine, Johns Hopkins University School of Medicine, Baltimore, Maryland

[e]Division of Cardiology, Department of Medicine, University of Anschutz Medical Campus, Aurora, Colorado

[f]Colorado Clinical and Translational Sciences Institute, University of Colorado Anschutz Medical Campus, Aurora, Colorado

[g]Division of Cardiology, Department of Medicine, Medical University of South Carolina, Charleston, South Carolina

Abstract

BACKGROUND: Detecting right heart failure post left ventricular assist device (LVAD) is challenging. Sensitive pressure-volume loop assessments of right ventricle (RV) contractility may improve our appreciation of post-LVAD RV dysfunction.

METHODS: Thirteen LVAD patients and 20 reference (non-LVAD) subjects underwent comparison of echocardiographic, right heart cath hemodynamic, and pressure-volume loop-

Reprint requests: Steven Hsu, MD, Division of Cardiology, Johns Hopkins Medical Institutions, 1800 Orleans Street Zayed 7125S, Baltimore, MD 21287. Telephone: (410) 502-0955. steven.hsu@jhmi.edu.

[1]@Js08Paul.

[2]Twitter: @stevenhsu_md.

Author contributions

PJS and SH developed concept, designed study, performed procedures, analyzed data, and drafted manuscript. IMCS, SF, LH, MK, and AW collected and processed data, refined study design. MM performed procedures and collected data. PMH, WKC, and RJT designed and refined study. PJS, IMCS, MM, FA, NAG, KS, AK, PAH, RJT, and SH performed critical review of the manuscript and revised accordingly.

derived assessments of RV contractility using end-systolic elastance (Ees), RV afterload by effective arterial elastance (Ea), and RV-pulmonary arterial coupling (ratio of Ees/Ea).

RESULTS: LVAD patients had lower RV Ees (0.20 ± 0.08 vs 0.30 ± 0.15 mm Hg/ml, $p = 0.01$) and lower RV Ees/Ea (0.37 ± 0.14 vs 1.20 ± 0.54, $p < 0.001$) versus reference subjects. Low RV Ees correlated with reduced RV septal strain, an indicator of septal contractility, in both the entire cohort ($r = 0.68$, $p = 0.004$) as well as the LVAD cohort itself ($r = 0.78$, $p = 0.02$). LVAD recipients with low RV Ees/Ea (below the median value) demonstrated more clinical heart failure (71% vs 17%, $p = 0.048$), driven by an inability to augment RV Ees (0.22 ± 0.11 vs 0.19 ± 0.02 mm Hg/ml, $p = 0.95$) to accommodate higher RV Ea (0.82 ± 0.38 vs 0.39 ± 0.08 mm Hg/ml, $p = 0.002$). Pulmonary artery pulsatility index (PAPi) best identified low baseline RV Ees/Ea (≤0.35) in LVAD patients ((area under the curve) AUC = 0.80); during the ramp study, change in PAPi also correlated with change in RV Ees/Ea ($r = 0.58$, $p = 0.04$).

CONCLUSIONS: LVAD patients demonstrate occult intrinsic RV dysfunction. In the setting of excess RV afterload, LVAD patients lack the RV contractile reserve to maintain ventriculo-vascular coupling. Depression in RV contractility may be related to LVAD left ventricular unloading, which reduces septal contractility.

Keywords

right heart failure; left ventricular assist device; pressure-volume loop; echocardiographic strain; pulmonary hypertension

Late right heart failure (RHF) is emerging as a vexing complication following left ventricular assist device (LVAD) implantation.[1–5] Its relative importance is increasing as rates of post-LVAD hemocompatibility-related adverse events have fallen in recent years.[2] Overall rates of postoperative RHF have remained unchanged post-LVAD[2,6–8] and have even increased in the case of late RHF.[9] The definition of late RHF, refined in 2020,[10] relies on RHF hospitalization, thereby rendering it rather specific. Many more LVAD recipients suffer as outpatients with right-sided congestive symptoms and end-organ consequences that worsen quality of life, longevity, and successful bridging to transplant.[8,11] Detection of RHF post-LVAD also relies on clinical, echocardiographic, and hemodynamic assessments of right ventricle (RV) function that are dynamic and load-dependent. Thus, their poor sensitivity for detecting intrinsic RV dysfunction in its earlier stages[1,12] limits our ability to identify and prevent late RHF before it becomes manifest.

A better accounting of the full extent of intrinsic RV function in LVAD recipients would improve the diagnosis, prevention, and ultimate treatment of RHF post-LVAD. Invasive RV pressure-volume loop measurements provide a potential methodology to address this need. Pressure-volume loops facilitate assessment of RV end-systolic elastance (Ees), a highly sensitive, load-independent measure of RV contractility, as well as effective arterial elastance (Ea), which enables the calculation of right ventricular-vascular coupling as the ratio of Ees/Ea.[13] Our group[14–17] and others[18] have leveraged invasive pressure-volume loop measurements of RV Ees and Ees/Ea to uncover occult RV dysfunction. In the present study, we prospectively measure RV pressure-volume loop measurements alongside clinical indices in a cohort of LVAD recipients and compare them to those of non-LVAD reference subjects

to assess the full extent of LVAD RV contractile dysfunction. In doing so, we uncover new insights into intrinsic RV contractility, contractile reserve, and vascular coupling in LVAD patients that shed light on the extent and possible etiologies of intrinsic RV dysfunction in the LVAD population.

Materials and methods

Study population

LVAD patients at least 1 month after implantation referred for right heart catheterization (RHC) were prospectively enrolled at a single LVAD center between 2021 and 2022. Referral reason was categorized as either for assessment of heart failure symptoms or for routine hemodynamic assessment. Non-LVAD reference subjects underwent RHC at 3 centers (Johns Hopkins University, Colorado University, Medical University of South Carolina). Reference subjects were comprised of generally healthy subjects free of cardiopulmonary disease. They did not meet criteria for heart failure (pulmonary capillary wedge pressure [PCWP] > 15 mm Hg) or pulmonary hypertension (mean pulmonary artery pressure [mPAP] > 20 mm Hg). Institutional review boards at each center approved all studies. All patients provided written informed consent.

Study design

All patients underwent prospective clinical assessment at the time of RHC paired with laboratory assessment obtained either same day or within 1 month prior. All underwent 8 Fr venous access under local anesthetic via the right internal jugular vein followed by clinical RHC in the supine position. LVAD patients also underwent additional RHC and echocardiographic assessments at additional LVAD speeds (measured after 2 minutes at the new speed). Appropriate low, medium, and high speeds were chosen for each patient, unless otherwise noted. HeartWare (Medtronic, Minneapolis, MN) and HeartMate 3 (Abbott, Chicago, IL) LVAD patients underwent 100 and 200 rpm increment changes, respectively.

Routine hemodynamic pressure measurements were obtained at end-expiration while cardiac outputs were based on the average of 3 thermodilution measurements with < 10% error. Additional hemodynamic indexes of RV function were calculated as follows:

$$\text{Pulmonary artery pulsatility index (PAPi)} = (\text{sPAP} - \text{dPAP})/\text{RAP} \quad (1)$$

$$\text{Pulmonary artery compliance (PAC)} = \text{SV}/(\text{sPAP} - \text{dPAP}) \quad (2)$$

$$\text{RV stroke work index (RVSWI)} = 0.136(\text{SVI})(\text{mPAP} - \text{RAP}) \quad (3)$$

Above, sPAP is systolic pulmonary artery pressure, dPAP is diastolic pulmonary artery pressure, mPAP is mean pulmonary artery pressure, RAP is right atrial pressure, SV is stroke volume, and SVI is stroke volume index (SV normalized to body surface area). Parameter changes as a function of LVAD speed were calculated by subtracting the parameter of interest at the lowest recorded speed from the same parameter at the highest recorded speed.

Following completion of clinical RHC, the pulmonary artery catheter was replaced by a pressure-volume conductance pigtail catheter (CA-71103-PL or CA-41103-PN, CD Leycom, Netherlands) positioned in the RV apex under fluoroscopic guidance. Steady-state pressure-volume loop measurements at end-expiration were obtained at baseline for both groups, then at each LVAD speed for LVAD patients. Again, between each speed change, a 2-minute wait was observed with care to ensure the patient reached the same flow, power, and LVAD pulsatility observed at each speed during the clinical study.

Pressure-volume loop analysis

Volume signals from each segment were assessed using the Inca system and ConductNT software (CD Leycom, The Netherlands). Intracavitary segments with counter-clockwise pressure-volume signals were summed to yield total RV volume. Steady-state RV pressure-volume loops were calculated across 5 end-expiratory beats. RV Ees is ideally determined as the slope of the line connecting end-systolic points (ESP) as RV preload is reduced by inferior vena cava balloon occlusion or Valsalva maneuver.[13] However, the former would have added procedural risk while the latter could not be reliably performed on LVAD recipients. Instead, we calculated RV Ees using the well-described steady-state, single-beat method.[19,20] RV Ees was calculated as the difference between the modeled isovolumic beat peak pressure and the measured ESP divided by stroke volume. Meanwhile, RV Ea was defined as ESP divided by SV.

Echocardiogram strain analysis

Only patients at 1 center (Hopkins) had an echocardiogram done at the time of RHC. RV speckle-tracking echocardiographic-based strain analysis was performed offline using commercially available strain software (Epsilon EchoInsight Version 3.1.0.3358, Milwaukee, WI). From the apical 4-chamber view, peak systolic longitudinal strain of the RV free wall and septum was obtained in accordance with standard clinical practice and prior published work.[21] A board-certified echocardiologist (M.M.) performed all strain analyses blinded to all clinical and research-derived variables.

Statistical analysis

Categorical variables are represented as n (%) and continuous variables as mean ± standard deviation. They were compared using chi-square and Wilcoxon rank sum tests, respectively. To assess the relationship between pressure-volume loop-derived measures and echocardiographic or hemodynamic parameters, univariable linear regression was performed. A change in measurement was defined as the difference between its value at the high- and low-speed categories. To account for variable LVAD speeds tested in different patients, 3 ramp speed categories (low, medium, and high) were defined for each patient to assess the effect of speed change on dependent variables of interest. Not all patients

underwent 3 speeds, however; some only underwent 2 speed changes, with fewer speed changes occurring at random. Then, a repeated-measures analysis of variance was used to examine the effects of LVAD speed, patient group, as well as their interaction term (i.e., the differential effect of speed on each group) on various dependent variables of interest such as contractility or coupling. Area under receiver operating characteristic curves were used to determine the ability of clinical RHC parameters to predict low baseline RV Ees/Ea and negative Ees/Ea change between high and low speeds. Data were analyzed using STATA 17.0 (StataCorp, College Station, TX) and GraphPad Prism 9.4.1 (GraphPad, San Diego, CA). Statistical significance was defined by a 2-sided p-value < 0.05.

Results

Subject demographics

Thirty-three patients underwent RHC and RV pressure-volume loop measurements: 13 LVAD and 20 reference subjects. All had analyzable pressure-volume loop data. Patient demographic and clinical data are presented in Table 1. LVAD patients were predominantly male with mean age of 54 years. Among LVAD patients, the cause of the cardiomyopathy was primarily nonischemic (10/13, 77%). HeartMate 3 (69%) or HeartWare (31%) LVAD was implanted, most via full sternotomy (92%), between October 2015 and December 2021, a mean of 861 days (range 109-2,406) before pressure-volume loop measurement. Reference subjects differed from LVAD patients in that they were mostly female. The groups did not differ statistically with regards to age.

Hemodynamic comparison

RHC parameters are in Table 1. LVAD patients had higher right-sided, pulmonary, and left-sided pressures when compared to the reference group. Cardiac index and SV were both lower. LVAD patients had higher natriuretic peptide levels and serum creatinine. Among the calculated hemodynamic indexes of RV function, PAPi was different between the 2 groups (Table 1).

RV pressure-volume derived hemodynamic comparison

Representative pressure-volume loops for each group are shown in Figure 1A. LVAD patients had lower intrinsic RV contractility as assessed by single-beat-derived RV Ees compared to NCD patients (0.20 ± 0.08 vs 0.30 ± 0.15 mm Hg/ml, $p = 0.01$). This is combined with a higher total pulmonary arterial afterload, as indexed by RV Ea in LVAD patients (0.62 ± 0.35 vs 0.29 ± 0.14 mm Hg/ml, $p < 0.001$). Thus, there was reduced ventricular-vascular coupling, as indexed by RV Ees/Ea, in the LVAD patients (0.37 ± 0.14 vs 1.20 ± 0.54, $p < 0.001$) (Figure 1B).

Echo strain data

In the subset of patients with echo data, strain was analyzed whenever possible for both groups. LVAD patients had significantly worse RV strain than NCD patients, whether measured in the septum or free wall (Figure 2A-B), corresponding with the lower RV Ees seen in LVAD. Studies have hypothesized that the interventricular septal contribution to RV contractility may be diminished in LVAD patients due to left ventricular (LV) unloading by

the LVAD.[22] We therefore investigated whether RV Ees correlated to either septal strain, free wall strain, or both. Across both groups, RV Ees correlated significantly with RV septal strain but not RV free wall strain (Figure 2C-D). Further, this correlation held true even when looking at the LVAD cohort alone (Figure 2E-F).

LVAD RV contractility and ventricular-vascular coupling

To investigate the impact of reduced ventricular-vascular coupling among our LVAD patients, we dichotomized our group based on median baseline RV Ees/Ea (Ees/Ea > 0.35 vs ≤0.35). Demographic and clinical data for the 2 LVAD subgroups are shown in Table 2. There was a trend ($p = 0.10$) toward higher daily diuretic requirement in the low Ees/Ea ≤0.35 group. The reason for RHC referral was also different: Significantly more LVAD patients with low Ees/Ea were suffering from overt clinical heart failure symptoms (p=0.048). The lower coupling group also had higher pulmonary and biventricular filling pressures (Table 2). PAPi trended lower ($p = 0.08$) in the low coupling group, but other hemodynamic measures of RV contractility, compensation, and overall flow were not dramatically different between groups. Summed afterload (RV Ea) was significantly higher in the low coupling group (0.82 ± 0.38 vs 0.39 ± 0.08 mm Hg/ml, $p = 0.002$). Despite the higher afterload in the low coupling group, RV Ees did not increase to match Ea (Table 2), hence the lower Ees/Ea ratio in that group by definition.

We next sought to identify clinical RHC parameters that identified right ventricle-pulmonary arterial (RV-PA) uncoupling in LVAD patients. PAPi and CI correlated with RV Ees/Ea, the latter more weakly (Figure 3A). RVSWI and RAP/PCWP ratio did not. Based on area under the receiver operator curve analysis, there was a trend toward PAPi being able to predict RV Ees/Ea ≤0.35 ((area under the curve) AUC = 0.80, $p = 0.07$) (Figure 3B).

Changes in RV contractility and ventriculo-vascular coupling as a function of speed

With a speed increase, RV Ea declined slightly (Figure 4). RV Ees, however, behaved differently with respect to speed increases. In the higher coupling group, Ees rose with speed increase; in the poor coupling group, however, Ees actually declined with speed increase (interaction $p = 0.05$) (Figure 4). This behavior drove a significant group difference in Ees/Ea behavior with respect to speed (interaction $p = 0.02$) (Figure 4). Among clinical parameters of RV function, only a change in PAPi was correlated with an increase in Ees/Ea with speed increase (Figure 5A). Based on area under receiver operator characteristic analysis, change in PAPi performed best (AUC = 0.76) at predicting an improvement in RV Ees/Ea. This relationship, however, was not statistically significant ($p = 0.12$) (Figure 5B).

Discussion

In the present study, we leveraged RV pressure-volume loop measurements to assess load-independent RV contractility in LVAD patients versus non-LVAD reference subjects. We found that LVAD patients have depressed intrinsic RV contractility as assessed by Ees and reduced RV compensation as indexed by RV-PA coupling. Reduced RV Ees was correlated specifically with reduced septal strain, suggesting that LV unloading may play an important role in septal contractility and, in turn, chamber-level RV contractility. Those LVAD patients

with the worst RV-PA coupling demonstrated more signs and symptoms of clinical heart failure, in association with an inability to augment RV contractility in the face of increased afterload. During LVAD speed changes, disparate behavior in RV Ees/Ea was mostly driven by different behavior in RV Ees. PAPi, both at baseline and with speed changes, provided the best proxy for RV Ees/Ea. Our results provide new insights into the prevalence of intrinsic RV contractile dysfunction in LVAD patients and highlight the important roles that the septum and summed pulmonary afterload may play on RV contractility and RV-vascular coupling in the setting of LVAD physiology.

Occult RV dysfunction in LVAD recipients

Slight decrements to RV contractility in the setting of increased pulmonary afterload are hard to detect.[1,23] Standard echocardiographic and hemodynamic measures of RV function can miss occult RV dysfunction.[17] Here, we demonstrate that intrinsic RV contractility is much lower in LVAD patients than previously thought. Our low RV Ees values (0.23 ± 0.10 mm Hg/ml) are lower than, but not statistically different from, prior published LVAD RV Ees values as reported by Brener and colleagues[24] (0.50 + 0.32 mm Hg/ml) and Tran and colleagues[25] (0.37 ± 0.14 mm Hg/ml). Interestingly, RV Ees was significantly low in all LVAD patients, even though half were asymptomatic. This highlights the potential existence of occult RV contractile dysfunction even among seemingly well-compensated LVAD patients.

Low RV contractility (Ees) became a major issue among LVAD patients with high afterload (Ea). In the face of higher Ea, we found that LVAD patients seemed to lack any RV reserve to increase Ees and preserve the Ees/Ea ratio. This lack of RV reserve was reminiscent of that seen in adult congenital heart disease patients with Fontan physiology[26] or group I pulmonary arterial hypertension patients with RV failure.[17,27] LVAD patients have previously been shown to have poor RV reserve during exercise.[25,27,28] Among LVAD patients, the RV shows some initial contractile reserve but quickly fails to augment contractility in the face of ongoing increases in exertional afterload.[25] By showing that this issue is even present at rest and also present among asymptomatic individuals, this study suggests that poor intrinsic RV contractility among LVAD patients may be more prevalent than previously appreciated.

Influence of septal contractility

LV septal contractility contributes significantly to intrinsic RV contractility, a finding discovered over 30 years ago.[29] This is relevant in LVAD patients, since significant LV unloading reduces LV preload, stroke work,[22] and thus septal contractility. Since RV septal strain approximates septal contractility, we tested for and found a significant correlation between RV septal strain and RV Ees. Moreover, RV Ees was only correlated to RV septal strain and not free wall strain, suggesting a specific and stronger relationship between the septum and RV contractility. To our knowledge, this is the first study specifically examining septal strain and RV Ees; prior studies focused only on LVAD global or free-wall RV strain.[30] Although we do not prove a causative relationship between RV septal contractility and RV Ees, our ramp data did reveal that in patients with poor Ees/Ea, further increases in LVAD speed actually decreased RV Ees, perhaps by further reducing septal contractility.

Surgical technique may also affect RV function,[31] since sternotomy and the resultant loss of pericardial restraint may influence RV geometry and septal function, especially with intrapericardial pumps.[31] Unfortunately, the predominantly full-sternotomy approach among our patients limited the study of sternotomy versus sternotomy-sparing surgical approaches. Further studies should test the causative relationship between LVAD unloading, septal contractility, surgical technique, and RV Ees.

Right ventricular-vascular coupling

Our results suggest that, among LVAD patients with poor RV reserve, small increases in pulmonary arterial afterload may have a more deleterious effect. This matches prior work by us and others showing that residual high pulmonary vascular resistance post-LVAD correlates with late RHF[9] and an increased diastolic pulmonary gradient correlates with worse outcomes.[32] Of note, it remains unclear in LVAD patients whether a high DPG causes RV failure or vice versa. A persistently high DPG could represent pathologic pulmonary vascular remodeling that worsens RV function. However, only 1 LVAD patient in our cohort had a DPG > 5 mm Hg at baseline, pointing to additional contributory factors. In an LVAD patient, increasing the LVAD speed in a patient with intrinsic RVF could cause LV suction, lower PCWP, and thereby exacerbate the DPG. In fact, this exact behavior was seen in a study by Imamura and colleagues.[32] That said, an LVAD speed that is too low has equally deleterious consequences,[33,34] leading to excess heart failure hospitalizations and less chance of myocardial recovery.[35] Future studies are needed to better determine the relationship between LVAD RV failure and DPG and the best way to balance LVAD speed with RV contractile function. A better understanding of these mechanisms should also refine LVAD patient selection for oral pulmonary vasodilators, which do indeed show benefit in some LVAD patients, as recently described by Xanthopoulos and colleagues.[36]

Measuring pressure-volume loops remains impractical in routine clinical practice. Here, we correlate for the first time RV pressure-volume loop parameters to standard clinical indexes. By doing so, we find that PAPi may prove to be a useful correlate of RV Ees/Ea in LVAD recipients. This finding matches the utility PAPi has shown in several clinical arenas including advanced heart failure and LVAD patients[37] and has even shown a correlation to intrinsic RV myocyte failure.[38] Future studies should ascertain whether PAPi is indeed a useful correlate of pressure-volume loop-derived Ees/Ea.

This study has several limitations. As a single-center study, applicability may be limited due to center-specific LVAD management. However, our observed RV Ees values were similar to 2 other studies of RV Ees in LVAD recipients.[24,25] Our limited cohort size, although similar to or larger than any prior RV pressure-volume loop studies of LVAD patients,[24,25] may have introduced type II error. Similarly, strain analysis could not be performed universally due to inadequate echocardiographic image quality, further reducing the cohort size for strain analyses. Sex differences between our LVAD and reference cohort may have led to a lower Ees among the LVAD group, but they would not have affected our analyses of the LVAD patient cohort itself. The use of repeated-measures analysis of variance assumes any missing ramp speeds were missing at random, which they were; however, effect estimates may be biased if the missing values were systematically different from observed values.

In conclusion, LVAD patients have significantly lower intrinsic RV contractility than previously appreciated. In the face of increased afterload, LVAD patients also demonstrate poor RV reserve and reduced RV-vascular coupling, leading to clinical heart failure. Poor intrinsic RV contractility in LVAD patients correlates to reduced septal strain. Given the importance of LV septal contractility to intrinsic RV contractility, this suggests a potential causative role of LVAD LV unloading on RV contractility. Lastly, PAPi may be a suitable clinical surrogate of poor RV-vascular coupling as measured by RV pressure-volume loops. Our study suggests RV contractility in LVAD patients may be much worse than previously appreciated and offers several potential new lines of investigation.

Financial support

There are no relevant financial disclosures relevant to this work.

References

1. Ali H, Kiernan M, Choudhary G, et al. Right ventricular failure post-implantation of left ventricular assist device: prevalence, pathophysiology, and predictors. ASAIO J 2020;66:610–9. 10.1097/MAT.0000000000001088. ⟨https://www.ncbi.nlm.nih.gov/pubmed/31651460⟩. [PubMed: 31651460]
2. Mehra MR, Goldstein DJ, Cleveland JC, et al. Five-year outcomes in patients with fully magnetically levitated vs axial-flow left ventricular assist devices in the MOMENTUM 3 randomized trial. JAMA 2022;328:1233–42. https://doi.org/10.1001/jama.2022.16197. ⟨https://dx.doi.org/10.1001/jama.2022.16197⟩. [PubMed: 36074476]
3. Rogers JG, Pagani FD, Tatooles AJ, et al. Intrapericardial left ventricular assist device for advanced heart failure. N Engl J Med 2017;376:451–60. 10.1056/NEJMoa1602954⟨10.1056/NEJMoa1602954⟨. [PubMed: 28146651]
4. Slaughter MS, Rogers JG, Milano CA, et al. Advanced heart failure treated with continuous-flow left ventricular assist device. N Engl J Med 2009;361:2241–51. 10.1056/NEJMoa0909938. ⟨http://content.nejm.org/cgi/content/abstract/361/23/2241⟩. [PubMed: 19920051]
5. Rajapreyar I, Soliman O, Brailovsky Y, et al. Late right heart failure after left ventricular assist device implantation. Jacc Heart Fail 2023;11:865–78. https://doi.org/10.1016/j.jchf.2023.04.014 ⟨https://dx.doi.org/10.1016/j.jchf.2023.04.014⟩. [PubMed: 37269258]
6. Kapelios CJ, Charitos C, Kaldara E, et al. Late-onset right ventricular dysfunction after mechanical support by a continuous-flow left ventricular assist device. J Heart lung Transplant 2015;34:1604–10. https://doi.org/10.1016/j.healun.2015.05.024. ⟨https://www.clinicalkey.es/playcontent/1-s2.0-S105324981501298X⟩. [PubMed: 26163154]
7. Rich JD, Gosev I, Patel CB, et al. The incidence, risk factors, and outcomes associated with late right-sided heart failure in patients supported with an axial-flow left ventricular assist device. J Heart Lung Transplant 2017;36:50–8. https://doi.org/10.1016/j.healun.2016.08.010. ⟨https://dx.doi.org/10.1016/j.healun.2016.08.010⟩. [PubMed: 27746085]
8. Takeda K, Takayama H, Colombo PC, et al. Incidence and clinical significance of late right heart failure during continuous-flow left ventricular assist device support. J Heart Lung Transplant 2015;34:1024–32. 10.1016/j.healun.2015.03.011. ⟨https://www.clinicalkey.es/playcontent/1-s2.0-S1053249815011079⟩. [PubMed: 25935438]
9. Alkhunaizi FA, Azih NI, Read JM, et al. Characteristics and predictors of late right heart failure after left ventricular assist device implantation. ASAIO J 2023;69:315–23. 10.1097/MAT.0000000000001804. ⟨https://www.narcis.nl/publication/RecordID/oai:pure.eur.nl:publications%2F23b9429c-7f81-41ae-aa33-abf30dcc2c12⟩. [PubMed: 36191552]
10. Kormos RL, Antonides CFJ, Goldstein DJ, et al. Updated definitions of adverse events for trials and registries of mechanical circulatory support: A consensus statement of the mechanical circulatory support academic research consortium. J Heart Lung Transplant 2020;39:735–50.

https://doi.org/10.1016/j.healun.2020.03.010. ⟨https://dx.doi.org/10.1016/j.healun.2020.03.010⟩. [PubMed: 32386998]

11. Rame JE, Pagani FD, Kiernan MS, et al. Evolution of late right heart failure with left ventricular assist devices and association with outcomes. J Am Coll Cardiol 2021;78:2294–308. 10.1016/j.jacc.2021.09.1362. ⟨https://www.ncbi.nlm.nih.gov/pubmed/34857091⟩. [PubMed: 34857091]
12. Bellavia D, Iacovoni A, Scardulla C, et al. Prediction of right ventricular failure after ventricular assist device implant: systematic review and metaanalysis of observational studies. Eur J Heart Fail 2017;19:926–46. 10.1002/ejhf.733. ⟨10.1002/ejhf.733⟩. [PubMed: 28371221]
13. Brener MI, Masoumi A, Ng VG, et al. Invasive right ventricular pressure-volume analysis: basic principles, clinical applications, and practical recommendations. Circ Heart Fail 2022;15:e009101. 10.1161/circheartfailure.121.009101. [PubMed: 34963308]
14. Alkhunaizi FA, Harowicz MR, Ireland CG, et al. Kussmaul's sign in pulmonary hypertension corresponds with severe pulmonary vascular pathology rather than right ventricular diastolic dysfunction. Circ Heart Fail 2021;14:e007461. 10.1161/CIRCHEARTFAILURE.120.007461. ⟨https://www.ncbi.nlm.nih.gov/pubmed/33356363⟩. [PubMed: 33356363]
15. Hsu S, Houston B, Tampakakis E, et al. Right ventricular functional reserve in pulmonary arterial hypertension. Circulation 2016;133:2413–22. 10.1161/aRCULATIONAHA.n6.022082. ⟨https://www.ncbi.nlm.nih.gov/pubmed/27169739⟩. [PubMed: 27169739]
16. Ireland CG, Damico RL, Kolb TM, et al. Exercise right ventricular ejection fraction predicts right ventricular contractile reserve. J Heart Lung Transplant 2021;40:504–12. https://doi.org/10.1016/j.healun.2021.02.005. ⟨https://dx.doi.org/10.1016/j.healun.2021.02.005⟩. [PubMed: 33752973]
17. Tedford RJ, Mudd JO, Girgis RE, et al. Right ventricular dysfunction in systemic sclerosis-associated pulmonary arterial hypertension. Circ Heart Fail 2013;6:953–63. 10.1161/aRCHEARTFAILURE.n2.000008. ⟨https://www.ncbi.nlm.nih.gov/pubmed/23797369⟩. [PubMed: 23797369]
18. Tello K, Richter MJ, Yogeswaran A, et al. Sex differences in right ventricular–pulmonary arterial coupling in pulmonary arterial hypertension. Am J Respir Crit Care Med 2020;202:1042–6. 10.1164/rccm.202003-0807LE. ⟨https://www.ncbi.nlm.nih.gov/pubmed/32501730⟩. [PubMed: 32501730]
19. Brimioulle S, Wauthy P, Ewalenko P, et al. Single-beat estimation of right ventricular end-systolic pressure-volume relationship. Am J Physiol Heart Circ Physiol 2003;284:1625–30. 10.1152/ajpheart.01023.002. ⟨http://ajpheart.physiology.org/content/284/5/H1625⟩.
20. Heerdt PM, Kheyfets V, Charania S, Elassal A, Singh I. A pressure-based single beat method for estimation of right ventricular ejection fraction: proof of concept. Eur Respir J 2020;55:1901635. 10.1183/13993003.01635-2019. ⟨https://www.ncbi.nlm.nih.gov/pubmed/31771999⟩. [PubMed: 31771999]
21. Mukherjee M, Mercurio V, Hsu S, et al. Assessment of right ventricular reserve utilizing exercise provocation in systemic sclerosis. Int J Cardiovasc Imaging 2021;37:2137–47. 10.1007/s10554-021-02237-9. ⟨https://link.springer.com/article/10.1007/s10554-021-02237-9⟩. [PubMed: 33860914]
22. Burkhoff D, Sayer G, Doshi D, Uriel N. Hemodynamics of mechanical circulatory support. J Am Coll Cardiol 2015;66:2663–74. 10.1016/j.jacc.2015.10.017. ⟨https://www.clinicalkey.es/playcontent/1-s2.0-S0735109715068990⟩. [PubMed: 26670067]
23. Houston BA, Shah KB, Mehra MR, Tedford RJ. A new twist on right heart failure with left ventricular assist systems. J Heart Lung Transplant 2017;36:701–7. 10.1016/j.healun.2017.03.014. ⟨https://www.clinicalkey.es/playcontent/1-s2.0-S1053249817317291⟩. [PubMed: 28416103]
24. Brener MI, Hamid NB, Fried JA, et al. Right ventricular pressure-volume analysis during LVAD speed optimization studies: insights into interventricular interactions and right ventricular failure. J Card Fail 2021;27:991–1001. ⟨https://www.ncbi.nlm.nih.gov/pubmed/33989781⟩. [PubMed: 33989781]
25. Tran T, Muralidhar A, Hunter K, et al. Right ventricular function and cardiopulmonary performance among patients with heart failure supported by durable mechanical circulatory support devices. J Heart Lung Transplant 2021;40:128–37. https://doi.org/10.1016/j.healun.2020.11.009. ⟨https://dx.doi.org/10.1016/j.healun.2020.11.009⟩. [PubMed: 33281029]

26. DeFaria Yeh D, Stefanescu Schmidt AC, Eisman AS, et al. Impaired right ventricular reserve predicts adverse cardiac outcomes in adults with congenital right heart disease. Heart (Br Card Soc) 2018;104:2044–50. https://doi.org/10.1136/heartjnl-2017-312572. ⟨http://dx.doi.org/10.1136/heartjnl-2017-312572⟩.
27. Ton V, Ramani G, Hsu S, et al. High right ventricular afterload is associated with impaired exercise tolerance in patients with left ventricular assist devices. ASAIO J 2021;67:39–45. 10.1097/MAT.0000000000001169. ⟨https://www.ncbi.nlm.nih.gov/pubmed/32412930⟩. [PubMed: 32412930]
28. Dorken Gallastegi A, Ergi GD, Kahraman ʊ, et al. Prognostic value of cardiopulmonary exercise test parameters in ventricular assist device therapy. ASAIO J 2022;68:808–13. 10.1097/MAT.0000000000001571. ⟨https://www.ncbi.nlm.nih.gov/pubmed/34494984⟩. [PubMed: 34494984]
29. Damiano RJ Jr, La Follette P Jr, Cox JL, Lowe JE, Santamore WP. Significant left ventricular contribution to right ventricular systolic function. Am J Physiol Heart Circ Physiol 1991;261:H1514–24. 10.1152/ajpheart.1991.261.5.h1514. ⟨http://ajpheart.physiology.org/cgi/content/abstract/261/5/H1514⟩.
30. Barssoum K, Altibi AM, Rai D, et al. Assessment of right ventricular function following left ventricular assist device (LVAD) implantation—the role of speckle-tracking echocardiography: a metaanalysis. Echocardiography (Mt Kisco, NY) 2020;37:2048–60. 10.1111/echo.14884. ⟨10.1111/echo.14884⟩.
31. Saeed D, Muslem R, Rasheed M, et al. Less invasive surgical implant strategy and right heart failure after LVAD implantation. J Heart Lung Transplant 2021;40:289–97. https://doi.org/10.1016/j.healun.2021.01.005. ⟨https://dx.doi.org/10.1016/j.healun.2021.01.005⟩. [PubMed: 33509653]
32. Imamura T, Chung B, Nguyen A, et al. Decoupling between diastolic pulmonary artery pressure and pulmonary capillary wedge pressure as a prognostic factor after continuous flow ventricular assist device implantation. Circ Heart Fail 2017;10:e003882. 10.1161/CIRCHEARTFAILURE.117.003882. ⟨https://www.ncbi.nlm.nih.gov/pubmed/28912260⟩. [PubMed: 28912260]
33. Uriel N, Burkhoff D, Rich JD, et al. Impact of hemodynamic ramp test-guided HVAD speed and medication adjustments on clinical outcomes. Circ Heart Fail 2019;12:e006067. 10.1161/CIRCHEARTFAILURE.119.006067. [PubMed: 30946600]
34. Uriel N, Sayer G, Addetia K, et al. Hemodynamic ramp tests in patients with left ventricular assist devices. Jacc Heart Fail 2016;4: 208–17. 10.1016/jochf.2015.10.001. ⟨https://www.clinicalkey.es/playcontent/1-s2.0-S2213177915006368⟩. [PubMed: 26746378]
35. Kanwar MK, Selzman CH, Ton V, et al. Clinical myocardial recovery in advanced heart failure with long term left ventricular assist device support. J Heart Lung Transplant 2022;41:1324–34. https://doi.org/10.1016/j.healun.2022.05.015. ⟨https://dx.doi.org/10.1016/j.healun.2022.05.015⟩. [PubMed: 35835680]
36. Xanthopoulos A, Wolski K, Wang Q, et al. Postimplant phosphodiesterase-5 inhibitor use in centrifugal flow left ventricular assist devices. Jacc Heart Fail 2022;10:89–100. https://doi.org/10.1016/j.jchf.2021.09.008. ⟨https://dx.doi.org/10.1016/j.jchf.2021.09.008⟩. [PubMed: 35115092]
37. Lim HS, Gustafsson F. Pulmonary artery pulsatility index: physiological basis and clinical application. Eur J Heart Fail 2020;22:32–8. 10.1002/ejhf.1679. ⟨10.1002/ejhf.1679⟩. [PubMed: 31782244]
38. Aslam MI, Jani V, Lin BL, et al. Pulmonary artery pulsatility index predicts right ventricular myofilament dysfunction in advanced human heart failure. Eur J Heart Fail 2021;23:339–41. [PubMed: 33347674]

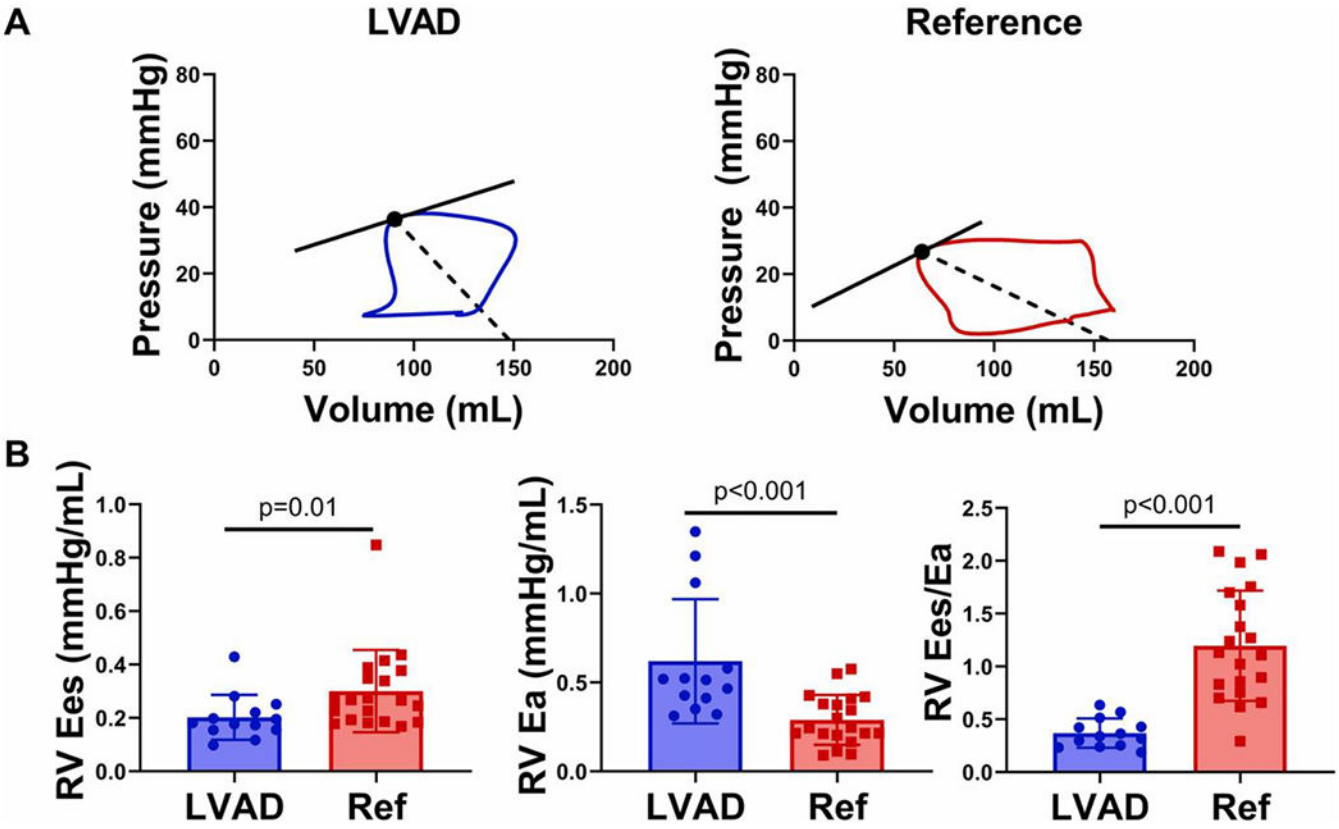

Figure 1.

RV contractility in LVAD patients. (A) Example pressure-volume loops for each group. RV Ees, solid line; Ea, dashed line. (B) RV contractility (Ees), afterload (Ea), and right ventricular-pulmonary arterial coupling (Ees/Ea) for each group. LVAD patients have lower intrinsic RV contractility and right ventricle-pulmonary arterial coupling, as indexed by Ees and Ees/Ea. Ea, effective arterial elastance; Ees, end-systolic elastance; LVAD, left ventricular assist device; RV, right ventricle.

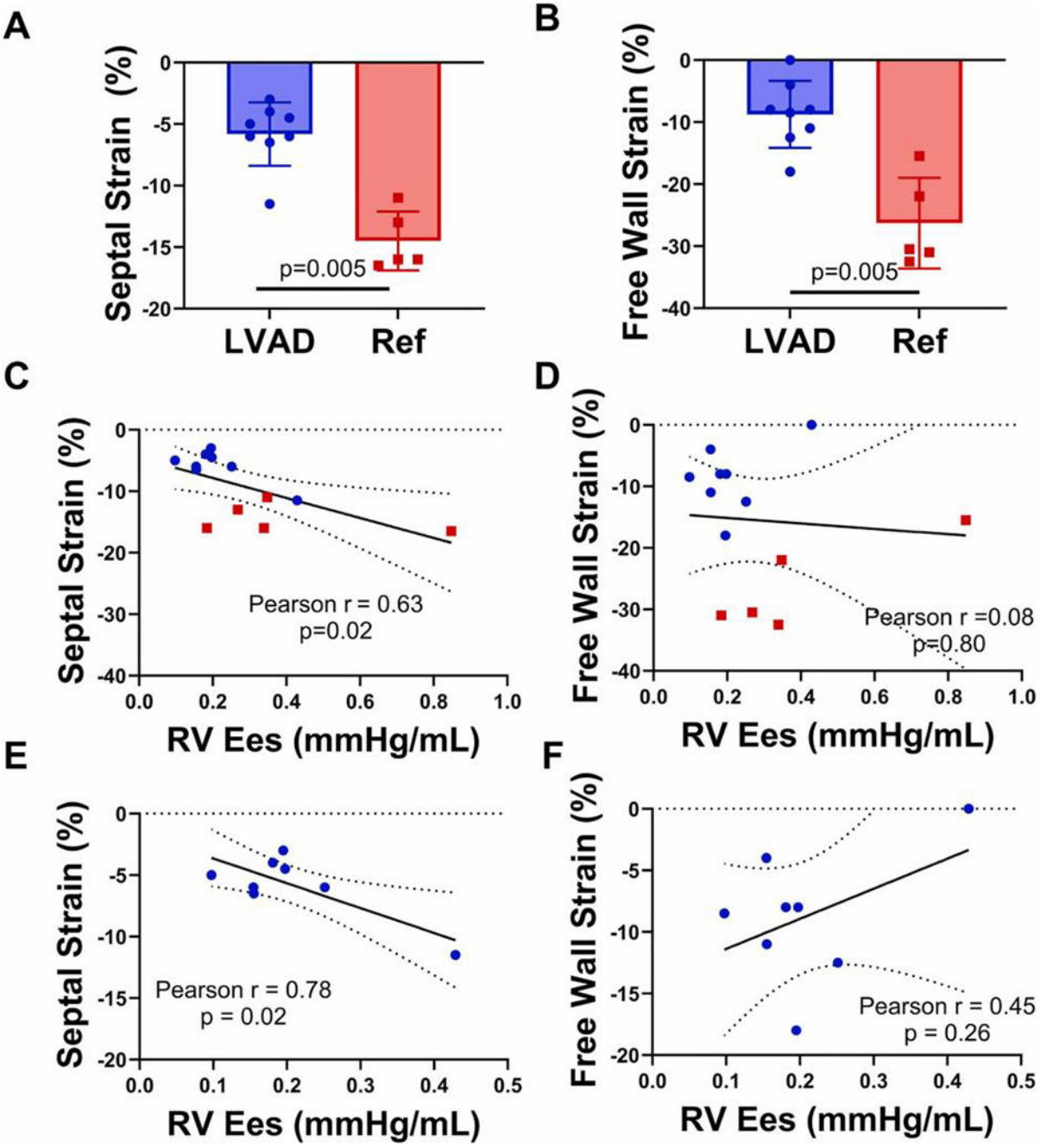

Figure 2.

Regional echocardiographic strain in LVAD and its relationship to chamber RV contractility. Both (A) RV septal strain and (B) RV free wall strain are significantly worse in LVAD versus controls. RV contractility as measured by Ees correlates with (C) RV septal strain but not (D) free wall strain. The specific correlation between RV Ees and septal strain, but not free wall strain, holds true even when looking at the LVAD cohort alone (E-F). Ees, end-systolic elastance; LVAD, left ventricular assist device; RV, right ventricle.

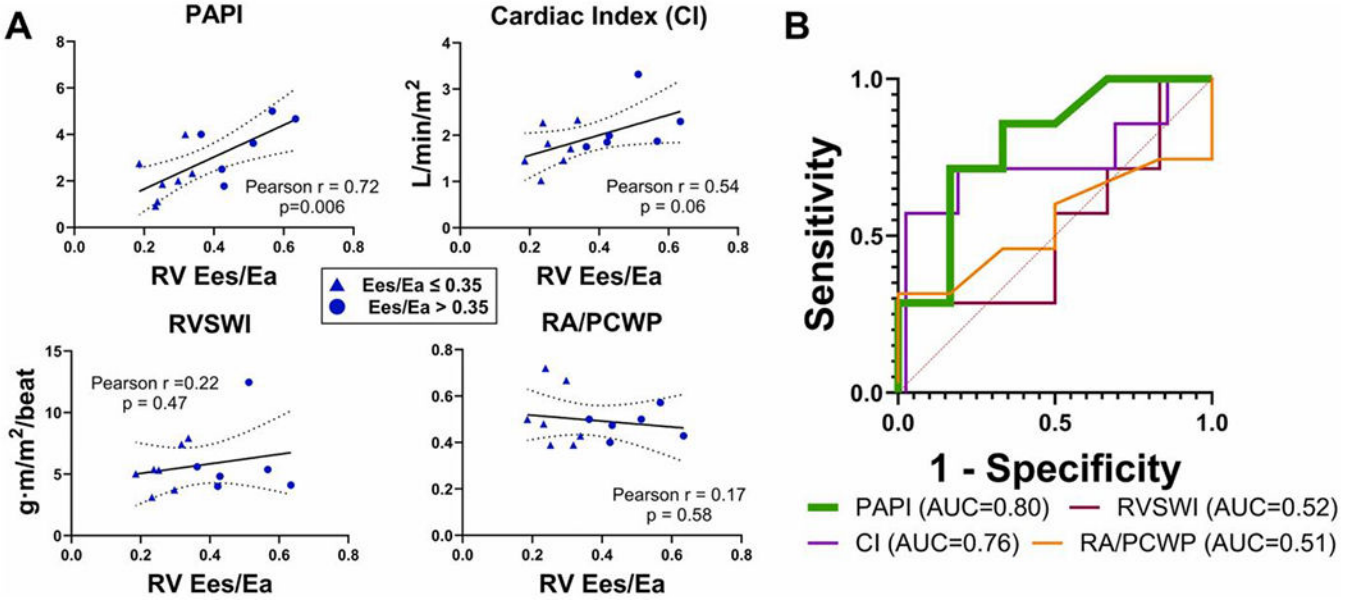

Figure 3.

Clinical surrogates of RV Ees/Ea. (A) Linear regressions of baseline right ventricle-pulmonary arterial coupling (Ees/Ea) versus select clinical indices of RV function. (B) Area under receiver operator characteristic curves for identifying poor right ventricle-pulmonary arterial coupling in an LVAD patients (Ees/Ea ≤0.35). PAPi and cardiac index correlate with Ees/Ea, while RVSWI and RA/ PCWP ratio do not. PAPi has the best AUROC for detecting depressed Ees/Ea. CI, cardiac index; Ea, effective arterial elastance; Ees, end-systolic elastance; LVAD, left ventricular assist device; PAPi, pulmonary artery pulsatility index; RA/PCWP, RA-to-pulmonary capillary wedge pressure; RV, right ventricle; RVSWI, right ventricular stroke work index.

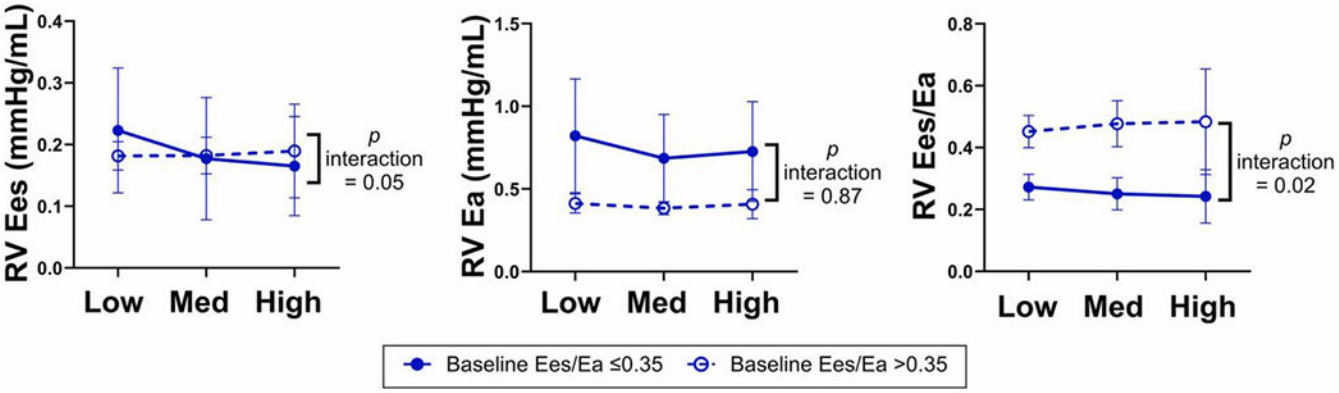

Figure 4.

RV contractility, afterload, and coupling as a function of left ventricular assist device (LVAD) speed. In LVAD patients with poor right ventricle-pulmonary arterial coupling, further increases in speed did reduce afterload but also reduced intrinsic RV contractility (Ees) more significantly than in patients with preserved coupling. As a result, poorly coupled patients saw a further decline in right ventricle-pulmonary arterial coupling at higher LVAD speeds (interaction $p = 0.02$). Ea, effective arterial elastance; Ees, end-systolic elastance; RV, right ventricle.

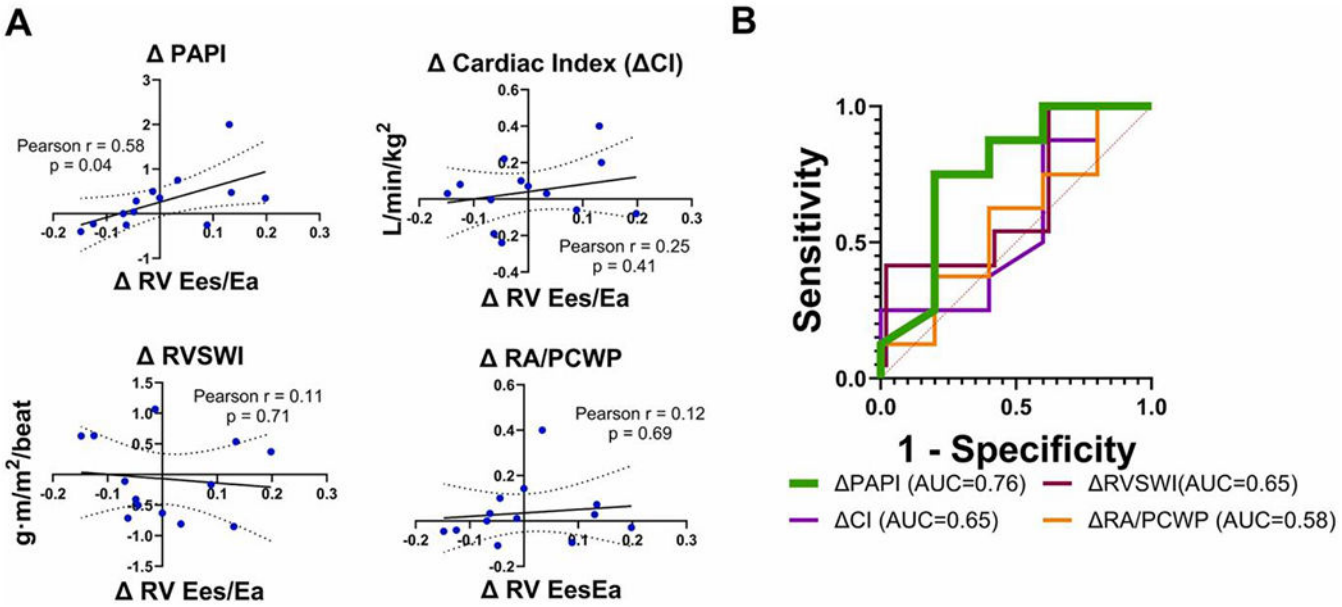

Figure 5.

Clinical surrogates of right ventricle-pulmonary arterial coupling change. (A) Linear correlations between clinical indices and the change in Ees/Ea with increasing speed. (B) Area under the receiver operator characteristic curves for predicting an improvement in Ees/ Ea at higher speed. Change in pulmonary artery pulsatility index was the only clinical parameter that correlated with change in Ees/Ea, showing reasonable discrimination for predicting an increase in Ees/Ea. Ea, effective arterial elastance; Ees, end-systolic elastance; PAPi, pulmonary artery pulsatility index; PCWP, pulmonary capillary wedge pressure; RV, right ventricle; RVSWI, right ventricular stroke work index.

Table 1

Clinical Characteristics and Hemodynamics of LVAD Versus Non-LVAD Reference Patients

Characteristic	LVAD (*n* = 13)	Reference (*n* = 20)	*p*-value
Women, *n* (%)	2 (15)	16 (90)	<0.001
Age (years)	54 ± 11	56 ± 16	0.60
Heart rate (min^{-1})	70 ± 18	69 ± 13	0.89
NT-proBNP (mg/dl) (reference *n* = 10)	1,501 ± 1,035	186 ± 155	<0.001
Creatinine (mg/dl) (reference *n* = 15)	1.5 ± 0.6	0.8 ± 0.4	<0.001
Right atrial pressure, RA (mm Hg)	8 ± 4	3 ± 1	<0.001
Systolic PAP (mm Hg)	38 ± 9	25 ± 5	<0.001
Diastolic PAP (mm Hg)	19 ± 7	9 ± 2	<0.001
Mean PAP (mm Hg)	25 ± 7	15 ± 3	<0.001
PCWP (mm Hg)	16 ± 6	7 ± 2	<0.001
Cardiac output (liter/min)	4.2 ± 1.2	5.6 ± 1.6	0.01
Cardiac index (liter/min per m^2)	1.9 ± 0.6	3.0 ± 0.7	<0.001
Stroke volume (ml)	55 ± 17	84 ± 33	<0.001
Pulmonary vascular resistance (Woods units)	2.2 ± 1.4	1.4 ± 0.7	0.01
Pulmonary artery pulsatility index (PAPI)	2.8 ± 1.3	5.8 ± 2.8	<0.001
Pulmonary artery compliance (ml/mm Hg)	2.9 ± 0.8	5.9 ± 3.7	0.001
Right ventricular stroke work index (RVSWI) ($g \cdot m/m^2$/beat)	5.7 ± 2.4	6.9 ± 2.8	0.19
RA/PCWP	0.5 ± 0.1	0.5 ± 0.2	0.11
Right ventricle end-systolic elastance (RV Ees) (mm Hg/ml)	0.20 ± 0.08	0.30 ± 0.15	0.01
Right ventricle effective arterial elastance (RV Ea) (mm Hg/ml)	0.62 ± 0.35	0.29 ± 0.14	<0.001
RV-PA coupling, RV Ees/Ea	0.37 ± 0.14	1.20 ± 0.54	<0.001

Abbreviations: LVAD, left ventricular assist device; NT-proBNP, N terminal-pro brain natriuretic peptide; PAP, pulmonary artery pressure; PCWP, pulmonary capillary wedge pressure; RV-PA, right ventricle-pulmonary arterial.

Table 2

Clinical, Echocardiographic, Hemodynamic, and Pressure-Volume-Derived Characteristics of LVAD Patients Split by Median RV Ees/Ea at Baseline Speed

Characteristic	Ees/Ea ≤0.35 (*n* = 7)	Ees/Ea > 0.35 (*n* = 6)	*p*-value
Women, *n* (%)	2 (29)	0 (0)	0.16
Ischemic etiology, *n* (%)	2 (29)	1 (17)	0.61
Sternotomy implant, *n* (%)	6 (86)	6 (100)	0.34
Left ventricle assist device (LVAD) type			0.85
Heartmate 3, *n* (%)	5 (71)	4 (80)	
HeartWare, *n* (%)	2 (29)	2 (20)	
Age (years)	54 ± 12	55 ± 10	1.0
Right heart catheterization referral reason			0.048
Clinical heart failure, *n* (%)	5 (71)	1 (17)	
Routine assessment, *n* (%)	2 (29)	5 (83)	
Daily diuretic requirement (furosemide equivalents)	77 ± 104	10 ± 17	0.10
Heart rate (min^{-1})	68 ± 22	72 ± 12	0.29
Mean arterial pressure (mm Hg)	81 ± 12	85 ± 13	0.60
Hemoglobin (g/dl)	11.7 ± 0.9	12.4 ± 0.8	0.07
Platelets (K/mm^3)	222 ± 76	177 ± 45	0.28
Sodium (mmol/liter)	138 ± 4	141 ± 3	0.14
Chloride (mmol/liter)	104 ± 2	105 ± 4	0.45
Blood urea nitrogen (mg/dl)	23 ± 10	23 ± 13	0.97
Creatinine (mg/dl)	1.4 ± 0.5	1.5 ± 0.7	0.81
Total bilirubin (mg/dl)	0.5 ± 0.2	0.6 ± 0.1	0.96
NT-proBNP (mg/dl)	1686 ± 889	1285 ± 1232	0.53
Lactate dehydrogenase, LDH (U/liter)	237 ± 105	195 ± 66	0.23
International normalized ratio (INR)	2.4 ± 0.3	2.3 ± 0.4	0.47
Baseline power (watts)	4.3 ± 0.5	4.5 ± 0.8	0.92
Baseline flow (liter/min)	4.1 ± 0.5	4.0 ± 0.7	0.92
LVEF, %	14 ± 5	18 ± 7	0.26
Mitral regurgitation ≥ moderate	1 (14)	0 (0)	0.34

Characteristic	Ees/Ea ≤0.35 (*n* = 7)	Ees/Ea > 0.35 (*n* = 6)	*p*-value
Tricuspid regurgitation ≥ moderate	2 (29)	0 (0)	0.16
Right atrial pressure (mm Hg)	10 ± 4	6 ± 2	0.04
Systolic PAP (mm Hg)	42 ± 9	34 ± 8	0.11
Diastolic PAP (mm Hg)	23 ± 6	14 ± 4	0.02
Mean PAP (mm Hg)	29 ± 6	21 ± 5	0.04
Pulmonary capillary wedge pressure (mm Hg)	20 ± 4	13 ± 5	0.03
Pulmonary artery saturation (%)	59.1 ± 7.3	64.2 ± 3.0	0.25
Cardiac output (liter/min)	3.8 ± 1.0	4.7 ± 1.3	0.19
Cardiac index (liter/min/m^2)	1.7 ± 0.5	2.2 ± 0.6	0.14
Stroke volume (ml)	47 ± 12	64 ± 19	0.10
Pulmonary vascular resistance (PVR) (Woods units)	2.7 ± 1.8	1.7 ± 0.7	0.29
Pulmonary artery pulsatility index (PAPi)	2.1 ± 1.0	3.6 ± 1.2	0.08
Pulmonary artery compliance (ml/mm Hg)	2.6 ± 0.9	3.3 ± 0.4	0.18
Right ventricular stroke work index (RVSWI) (g·m/m^2/beat)	5.4 ± 1.8	6.1 ± 3.2	0.94
RA/PCWP	0.5 ± 0.1	0.5 ± 0.1	0.97
Baseline right ventricle end-systolic elastance (RV Ees)	0.22 ± 0.11	0.19 ± 0.02	0.95
Baseline right ventricle arterial elastance (RV Ea)	0.82 ± 0.38	0.39 ± 0.08	0.002
Baseline RV-PA coupling, RV Ees/Ea	0.27 ± 0.05	0.49 ± 0.1	0.001

Abbreviations: LVAD, left ventricular assist device; LVEF, left ventricular ejection fraction; NT-proBNP, N terminal-pro brain natriuretic peptide; PAP, pulmonary artery pressure; PCWP, pulmonary capillary wedge pressure; RV-PA, right ventricle-pulmonary arterial.